

H.E.S.S. OBSERVATIONS OF THE GLOBULAR CLUSTERS NGC 6388 AND M15 AND SEARCH FOR A DARK MATTER SIGNAL

A. Abramowski¹, F. Acero², F. Aharonian^{3,4,5}, A. G. Akhperjanian^{5,6}, G. Anton⁷, A. Balzer⁷, A. Barnacka^{8,9}, U. Barres de Almeida^{10,35}, A. R. Bazer-Bachi¹¹, Y. Becherini^{12,13,36}, J. Becker¹⁴, B. Behera¹⁵, K. Bernlöhr^{3,16}, A. Bochow³, C. Boisson¹⁷, J. Bolmont¹⁸, P. Bordes¹⁹, V. Borrel¹¹, J. Brucker⁷, F. Brun¹³, P. Brun⁹, T. Bulik²⁰, I. Büsching²¹, S. Carrigan³, S. Casanova^{3,14}, M. Cerruti¹⁷, P. M. Chadwick¹⁰, A. Charbonnier¹⁸, R. C. G. Chaves³, A. Cheesebrough¹⁰, L.-M. Chounet¹³, A. C. Clapson³, G. Coignet²², J. Conrad²³, M. Dalton¹⁶, M. K. Daniel¹⁰, I. D. Davids²⁴, B. Degrange¹³, C. Deil³, H. J. Dickinson²³, A. Djannati-Atai^{12,36}, W. Domainko³, L. O' C. Drury⁴, F. Dubois²², G. Dubus²⁵, J. Dyks⁸, M. Dyrda²⁶, K. Egberts²⁷, P. Eger⁷, P. Espigat^{12,36}, L. Fallon⁴, C. Farnier², S. Fegan¹³, F. Feinstein², M. V. Fernandes¹, A. Fiasson²², G. Fontaine¹³, A. Förster³, M. Füßling¹⁶, Y. A. Gallant², H. Gast³, L. Gérard^{12,36}, D. Gerbig¹⁴, B. Giebels¹³, J. F. Glicenstein⁹, B. Glück⁷, P. Goret⁹, D. Göring⁷, S. Häffner⁷, J. D. Hague³, D. Hampf¹, M. Hauser¹⁵, S. Heinz⁷, G. Heinzlmann¹, G. Henri²⁵, G. Hermann³, J. A. Hinton²⁸, A. Hoffmann¹⁹, W. Hofmann³, P. Hofverberg³, M. Holler⁷, D. Horns¹, A. Jacholkowska¹⁸, O. C. de Jager²¹, C. Jahn⁷, M. Jamroz²⁹, I. Jung⁷, M. A. Kastendieck¹, K. Katarzyński³⁰, U. Katz⁷, S. Kaufmann¹⁵, D. Keogh¹⁰, D. Khangulyan³, B. Khélifi¹³, D. Klochkov¹⁹, W. Kluźniak⁸, T. Kneiske¹, Nu. Komin²², K. Kosack⁹, R. Kossakowski²², H. Laffon¹³, G. Lamanna²², D. Lennarz³, T. Lohse¹⁶, A. Lopatin⁷, C.-C. Lu³, V. Marandon^{12,36}, A. Marcowith², J. Masbou²², D. Maurin¹⁸, N. Maxted³¹, T. J. L. McComb¹⁰, M. C. Medina⁹, J. Méhault², R. Moderski⁸, E. Moulin⁹, C. L. Naumann¹⁸, M. Naumann-Godo⁹, M. de Naurois¹³, D. Nedbal³², D. Nekrassov³, N. Nguyen¹, B. Nicholas³¹, J. Niemiec²⁶, S. J. Nolan¹⁰, S. Ohm³, J.-P. Olive¹¹, E. de Oña Wilhelmi³, B. Opitz¹, M. Ostrowski²⁹, M. Panter³, M. Paz Arribas¹⁶, G. Pedalletti¹⁵, G. Pelletier²⁵, P.-O. Petrucci²⁵, S. Pita^{12,36}, G. Pühlhofer¹⁹, M. Punch^{12,36}, A. Quirrenbach¹⁵, M. Raue¹, S. M. Rayner¹⁰, A. Reimer²⁷, O. Reimer²⁷, M. Renaud², R. de los Reyes³, F. Rieger^{3,37}, J. Ripken²³, L. Rob³², S. Rosier-Lees²², G. Rowell³¹, B. Rudak⁸, C. B. Rulten¹⁰, J. Ruppel¹⁴, F. Ryde³³, V. Sahakian^{5,6}, A. Santangelo¹⁹, R. Schlickeiser¹⁴, F. M. Schöck⁷, A. Schulz⁷, U. Schwanke¹⁶, S. Schwarzbach¹⁹, S. Schwemmer¹⁵, M. Sikora⁸, J. L. Skilton³⁴, H. Sol¹⁷, G. Spengler¹⁶, Ł. Stawarz²⁹, R. Steenkamp²⁴, C. Stegmann⁷, F. Stinzing⁷, K. Stycz⁷, I. Sushch^{16,38}, A. Szostek^{25,29}, J.-P. Tavernet¹⁸, R. Terrier^{12,36}, O. Tibolla³, M. Tluczykont¹, K. Valerius⁷, C. van Eldik³, G. Vasileiadis², C. Venter²¹, J. P. Vialle²², A. Viana⁹, P. Vincent¹⁸, M. Vivier⁹, H. J. Völk³, F. Volpe³, S. Vorobiov², M. Vorster²¹, S. J. Wagner¹⁵, M. Ward¹⁰, A. Wiercholska²⁹, M. Zacharias¹⁴, A. Zajczyk⁸, A. A. Zdziarski⁸, A. Zech¹⁷, and H.-S. Zechlin¹

(HESS Collaboration)

¹ Universität Hamburg, Institut für Experimentalphysik, Luruper Chaussee 149, D-22761 Hamburg, Germany

² Laboratoire de Physique Théorique et Astroparticules, Université Montpellier 2, CNRS/IN2P3, CC 70, Place Eugène Bataillon, F-34095 Montpellier Cedex 5, France

³ Max-Planck-Institut für Kernphysik, P.O. Box 103980, D-69029 Heidelberg, Germany

⁴ Dublin Institute for Advanced Studies, 31 Fitzwilliam Place, Dublin 2, Ireland

⁵ National Academy of Sciences of the Republic of Armenia, Yerevan, Armenia

⁶ Yerevan Physics Institute, 2 Alikhanian Brothers St., 375036 Yerevan, Armenia

⁷ Universität Erlangen-Nürnberg, Physikalisches Institut, Erwin-Rommel-Str. 1, D-91058 Erlangen, Germany

⁸ Nicolaus Copernicus Astronomical Center, ul. Bartycka 18, 00-716 Warsaw, Poland

⁹ IRFU/DSM/CEA, CE Saclay, F-91191 Gif-sur-Yvette Cedex, France; emmanuel.moulin@cea.fr, jean-francois.glicenstein@cea.fr

¹⁰ Department of Physics, University of Durham, South Road, Durham DH1 3LE, UK

¹¹ Centre d'Etude Spatiale des Rayonnements, CNRS/UPS, 9 av. du Colonel Roche, BP 4346, F-31029 Toulouse Cedex 4, France

¹² Astroparticule et Cosmologie (APC), CNRS, Université Paris 7 Denis Diderot, 10 rue Alice Domon et Leonie Duquet, F-75205 Paris Cedex 13, France

¹³ Laboratoire Leprince-Ringuet, Ecole Polytechnique, CNRS/IN2P3, F-91128 Palaiseau, France

¹⁴ Institut für Theoretische Physik, Lehrstuhl IV: Weltraum und Astrophysik, Ruhr-Universität Bochum, D-44780 Bochum, Germany

¹⁵ Landessternwarte, Universität Heidelberg, Königstuhl, D-69117 Heidelberg, Germany

¹⁶ Institut für Physik, Humboldt-Universität zu Berlin, Newtonstr. 15, D-12489 Berlin, Germany

¹⁷ LUTH, Observatoire de Paris, CNRS, Université Paris Diderot, 5 Place Jules Janssen, 92190 Meudon, France

¹⁸ LPNHE, Université Pierre et Marie Curie Paris 6, Université Denis Diderot Paris 7, CNRS/IN2P3, 4 Place Jussieu, F-75252, Paris Cedex 5, France

¹⁹ Institut für Astronomie und Astrophysik, Universität Tübingen, Sand 1, D-72076 Tübingen, Germany

²⁰ Astronomical Observatory, The University of Warsaw, Al. Ujazdowskie 4, 00-478 Warsaw, Poland

²¹ Unit for Space Physics, North-West University, Potchefstroom 2520, South Africa

²² Laboratoire d'Annecy-le-Vieux de Physique des Particules, CNRS/IN2P3, 9 Chemin de Bellevue-BP 110 F-74941 Annecy-le-Vieux Cedex, France

²³ Oskar Klein Centre, Department of Physics, Royal Institute of Technology (KTH), Albanova, SE-10691 Stockholm, Sweden

²⁴ Department of Physics, University of Namibia, Private Bag 13301, Windhoek, Namibia

²⁵ Laboratoire d'Astrophysique de Grenoble, INSU/CNRS, Université Joseph Fourier, BP 53, F-38041 Grenoble Cedex 9, France

²⁶ Instytut Fizyki Jądrowej PAN, ul. Radzikowskiego 152, 31-342 Kraków, Poland

²⁷ Institut für Astro- und Teilchenphysik, Leopold-Franzens-Universität Innsbruck, A-6020 Innsbruck, Austria

²⁸ Department of Physics and Astronomy, The University of Leicester, University Road, Leicester, LE1 7RH, UK

²⁹ Obserwatorium Astronomiczne, Uniwersytet Jagielloński, ul. Orła 171, 30-244 Kraków, Poland

³⁰ Toruń Centre for Astronomy, Nicolaus Copernicus University, ul. Gagarina 11, 87-100 Toruń, Poland

³¹ School of Chemistry & Physics, University of Adelaide, Adelaide 5005, Australia

³² Charles University, Faculty of Mathematics and Physics, Institute of Particle and Nuclear Physics, V Holešovičkách 2, 180 00 Prague 8, Czech Republic

³³ Oskar Klein Centre, Department of Physics, Royal Institute of Technology (KTH), Albanova, SE-10691 Stockholm, Sweden

³⁴ School of Physics & Astronomy, University of Leeds, Leeds LS2 9JT, UK

Received 2011 February 11; accepted 2011 April 11; published 2011 June 8

ABSTRACT

Observations of the globular clusters (GCs) NGC 6388 and M15 were carried out by the High Energy Stereoscopic System array of Cherenkov telescopes for a live time of 27.2 and 15.2 hr, respectively. No gamma-ray signal is found at the nominal target position of NGC 6388 and M15. In the primordial formation scenario, GCs are formed in a dark matter (DM) halo and DM could still be present in the baryon-dominated environment of GCs. This opens the possibility of observing a DM self-annihilation signal. The DM content of the GCs NGC 6388 and M15 is modeled taking into account the astrophysical processes that can be expected to influence the DM distribution during the evolution of the GC: the adiabatic contraction of DM by baryons, the adiabatic growth of a black hole in the DM halo, and the kinetic heating of DM by stars. Ninety-five percent confidence level exclusion limits on the DM particle velocity-weighted annihilation cross section are derived for these DM halos. In the TeV range, the limits on the velocity-weighted annihilation cross section are derived at the $10^{-25} \text{ cm}^3 \text{ s}^{-1}$ level and a few $10^{-24} \text{ cm}^3 \text{ s}^{-1}$ for NGC 6388 and M15, respectively.

Key words: black hole physics – dark matter – gamma rays: general – globular clusters: individual (NGC 6388, M15)

Online-only material: color figure

1. INTRODUCTION

Dark matter (DM) is expected to play a key role in the dynamics of a wide range of systems, from galactic object scale to galaxy cluster scale (Bertone et al. 2005). The inner parts of galaxies were used extensively to search for DM even though they are not necessarily dominated by DM (Englmaier & Gerhard 2005). Observations by the High Energy Stereoscopic System (H.E.S.S.) experiment toward the Galactic Center reveal a very high energy (VHE; $E_\gamma \gtrsim 100 \text{ GeV}$) gamma-ray signal with the flux level $\Phi(> 1 \text{ TeV}) \approx 2 \times 10^{-12} \text{ cm}^{-2} \text{ s}^{-1}$ (Aharonian et al. 2009a). The plausible DM-originated fraction of this signal is entirely dominated by standard astrophysical emission processes (Aharonian et al. 2006a). As opposed to this, dwarf galaxies are believed to be among the most DM-dominated objects and are believed to have a reduced astrophysical background (Mateo 1998) since these objects have little or no recent star formation activity. Nearby dwarf galaxies in the Local Group have already been observed with H.E.S.S., i.e., Sagittarius, Canis Major, Sculptor, and Carina (Aharonian et al. 2008, 2009b, 2011), yielding no signal. Exclusion limits on the velocity-weighted annihilation cross section between $\sim 10^{-24}$ and $\sim 10^{-22} \text{ cm}^3 \text{ s}^{-1}$ have been reported in the TeV range.

Several Galactic globular clusters (GCs) have been observed with ground-based Cherenkov telescopes and upper limits on γ -ray emission from standard astrophysical processes have been reported on Omega Centauri, 47 Tucanae, M13, M15, and M5 (Kabuki et al. 2007; Aharonian et al. 2009c; Anderhub et al. 2009; McCutcheon 2009). GCs are also potential targets for indirect DM searches (Wood et al. 2008). They are dense stellar systems of $\gtrsim 10$ Gyr old, found in halos of galaxies, with typical masses between 10^4 and a few $10^6 M_\odot$, similar to dwarf galaxies. However, GCs are much more compact than dwarf galaxies. Observations of GCs do not suggest the presence of a significant amount of DM, but rather that these objects are dominated by baryons (Binney & Tremaine 1987). In the primordial formation scenario of GCs (Peebles 1984), GCs were formed in DM minihalos before or during

the reionization (Komatsu et al. 2009), before the formation of galaxies. However, the distribution of GC colors (Brodie & Strader 2006) suggests that only metal-poor clusters have a cosmological origin, while metal-rich clusters formed in star-forming events such as galaxy–galaxy mergers. The existence of an extended dark halo required by the GC primordial formation scenario has been challenged recently by Baumgardt et al. (2009) and Conroy et al. (2010). They show that the stellar kinematics of NGC 2419, a remote GC which experiences little tidal effects from the Milky Way, is incompatible with the presence of an extended dark halo. However, Cohen et al. (2010) have shown that the measured spread in the Ca abundance can be explained only if NGC 2419 is the remnant of a more massive object.

For the purpose of this paper, GCs are assumed to have formed in DM minihalos and thus were DM-dominated in their primordial stage. Note that M15 is a metal-poor GC, $[\text{Fe}/\text{H}] = -2.37$ (Harris 1996), while NGC 6388 is metal-rich, $[\text{Fe}/\text{H}] = -0.55$ (Harris 1996), so the DM minihalo scenario is better motivated for M15 than NGC 6388. However, NGC 6388 might host a $\gtrsim 10^3 M_\odot$ black hole (BH; Lanzoni et al. 2007). Such massive ($\gtrsim 10^3 M_\odot$) BHs are not easily formed in star-forming events (Yungelson et al. 2008) suggesting a primordial formation origin. During the evolution of the GC, the DM reacts to the infall of baryons and is pulled in toward the center. This process is usually referred to as the adiabatic contraction (AC) model (Blumenthal et al. 1986; Zel’dovich et al. 1980; Jesseit et al. 2002; Gnedin et al. 2004; Prada et al. 2004). The effect of the contraction of DM in response to the baryon infall is particularly important for the calculation of the DM annihilation in baryonic environments such as the Galactic Center region (Gnedin & Primack 2004; Prada et al. 2004).

The distribution of baryons and DM is affected by the kinetic heating of DM by baryons (Merritt 2004) and by the presence of a BH (Gondolo & Silk 1999). A growing body of observations on GCs shows that they may harbor intermediate-mass black holes (IMBHs) with masses ranging from 10^3 to $10^5 M_\odot$, although the existence of these objects is not yet established. Indirect evidence includes the extrapolation of the empirical relation $M_{\text{BH}}-M_{\text{Bulge}}$ found for the supermassive BHs in galactic nuclei, which leads naturally to the prediction of existence of IMBHs (Magorrian et al. 1998). Besides, ultra-luminous X-ray sources (ULXs) apparently not associated with active galactic nuclei are proposed to be related to IMBHs (Colbert & Ptak 2002; Swartz

³⁵ Supported by CAPES Foundation, Ministry of Education of Brazil, Brazil.

³⁶ Also at UMR 7164 (CNRS, Université Paris VII, CEA, Observatoire de Paris, France).

³⁷ European Associated Laboratory for Gamma-Ray Astronomy, jointly supported by CNRS and MPG.

³⁸ Supported by Erasmus Mundus, External Cooperation Window.

Table 1
List of H.E.S.S. Analysis Cuts (de Naurois & Rolland 2009)

Cut Name	γ -Event Cut Value
Shower goodness	$\diamond 0.4$
Image charge (photoelectrons)	120
Reconstructed shower depth (radiation length)	$[-1, 4]$
Reconstructed nominal distance ($^\circ$)	$\diamond 2$
Reconstructed event telescope multiplicity	2

Notes. The shower depth is the reconstructed primary interaction depth of the particle and the nominal distance is the angular distance of the image barycenter to the camera center.

et al. 2004; Dewangan et al. 2005). From the theoretical side, the existence of IMBHs is a generic assumption of scenarios that seek to explain the formation of supermassive BHs from the accretion and merging of massive seeds (Islam et al. 2004; Volonteri et al. 2003; Koushiappas et al. 2004). Several GCs may host IMBHs: NGC 6388 (Lanzoni et al. 2007), ω Centauri (Noyola et al. 2008) in the Milky Way or even G1 in M31 (Kong 2007; Ulvestad et al. 2007).

This paper is structured as follows. Section 2 describes the observations carried out with the H.E.S.S. experiment and the analysis of the data on the two Galactic GCs NGC 6388 and M15. In Section 3, the DM halo modeling relevant for the two GCs is briefly presented (more details are given in the Appendix) and exclusion limits on the velocity-weighted annihilation cross section of DM particles are derived for realistic DM halo profiles. Finally, the results are summarized in Section 4.

2. OBSERVATIONS AND DATA ANALYSIS

The H.E.S.S. array of Cerenkov telescopes is located in the Khomas Highland of Namibia at an altitude of 1800 m above sea level. The system consists of four Imaging Atmospheric Cerenkov telescopes of 12 m diameter ($\sim 107 \text{ m}^2$) each. The total field of view of H.E.S.S. is 5° in diameter. The H.E.S.S. instrument achieves an angular resolution of $5'$ per gamma-ray and a point-like source sensitivity at the level of $10^{-13} \text{ cm}^{-2} \text{ s}^{-1}$ above 1 TeV for a 5σ detection in 25 hr at an observation zenith angle of 20° (de Naurois & Rolland 2009).

For both M15 and NGC 6388, data are taken in *wobble mode* (Aharonian et al. 2006b), where the pointing direction is chosen at an alternating offset of ± 0.7 to ± 1.0 from the target position. Standard quality selection (Aharonian et al. 2006b) is applied to the data. After the calibration of the raw data from photomultiplier tube signals, the events are reconstructed using a technique based on a semi-analytical shower development model (de Naurois & Rolland 2009). This reconstruction method yields a relative energy resolution of $\sim 10\%$ and an angular resolution of 0.06 per gamma-ray (68% containment radius). The background level is estimated using the ring-background method (Pühlhofer et al. 2003; Berge et al. 2007). The core of the GCs is very small in comparison to the H.E.S.S. point-spread function. They would thus be seen as point sources by H.E.S.S. The source region, referred to hereafter as the ON region, is defined as a circular region of 0.07 radius around the target position. The background region is defined as an annulus around the pointing position with a medium radius equal to the distance of the target and a half-thickness of 0.07 . It is referred to hereafter as the OFF region. The cut values used to select the gamma-ray events are shown in Table 1. Given the Galactic latitude of the two Galactic GCs, contamination by diffuse TeV gamma-ray emission is very unlikely. The results

presented below have been cross-checked by an independent analysis chain (Berge et al. 2007; Aharonian et al. 2005). Both analyses give consistent results.

2.1. NGC 6388

NGC 6388 is one of the best known Galactic GC. It is located at ~ 11.5 kpc from the Sun, at R.A. = $17^{\text{h}}36^{\text{m}}17.05$ and decl. = $-44^\circ 44' 05.8$ (J2000), and has a mass estimated to be $\sim 10^6 M_\odot$. The stellar mass density in the core, with radius $r_c = 0.4$ pc (0.12 arcmin), reaches $\sim 5 \times 10^5 M_\odot \text{ pc}^{-3}$. The tidal radius is $r_t \sim 25$ pc (Lanzoni et al. 2007). The structural properties of NGC 6388 are summarized in Table 2. Using the high-resolution *Hubble Space Telescope* and Wide Field Imager observations at ESO, Lanzoni et al. (2007) show that the surface brightness density of stars significantly deviates from a flat core in the inner part, which is compatible with the existence of an IMBH with a mass of $\sim 5 \times 10^3 M_\odot$. A power law with a slope of -0.2 is detected in the surface brightness density profile, which suggests the presence of a central IMBH (Baumgardt et al. 2005; Noyola & Gebhardt 2006; Umbreit et al. 2008). The *Chandra* satellite has detected three X-ray sources, coincident in position with the center of gravity of NGC 6388 located with an uncertainty of 0.3 . One of these may be the X-ray counterpart of the putative IMBH (Nucita et al. 2008).

The H.E.S.S. observations of NGC 6388 were taken between 2008 June and 2009 July. The observation zenith angles range from 20° to 44° with a mean zenith angle of 22.9° , and the exposure time is 27.2 hr. The left-hand side of Figure 1 shows the θ^2 radial distribution of the ON and OFF events for NGC 6388. $N_{\text{ON}} = 71$ gamma-ray candidates were found in the ON region, while the measured number of OFF events is $N_{\text{OFF}} = 1754$. With the ratio of the off-source solid angle region to the on-source solid angle region $\alpha = 26.5$, the expected number of background events in the ON region is 66.1. Since N_{ON} and

N_{OFF}/α are compatible at the 2σ level, no significant gamma-ray excess is found above the background. An upper limit at 95% confidence level (C.L.) on the number of gamma-rays can be derived using the method developed in Rolke et al. (2005): $N_\gamma^{95\% \text{ C.L.}} = 21.6$.

2.2. M15

M15 (NGC 7078) is a well-studied Galactic GC centered at the position R.A. = $21^{\text{h}}28^{\text{m}}58.3$ and decl. = $12^\circ 10' 00.6$ (J2000). It is situated at ~ 10 kpc from the Sun. Its estimated mass is $\sim 5 \times 10^5 M_\odot$. The stellar mass density in the core with radius $r_c = 0.04$ pc is about $10^7 M_\odot \text{ pc}^{-3}$ (Dull et al. 1997), and the tidal radius is $r_t \sim 30$ pc. The structural properties of M15 are summarized in Table 2. The surface brightness density of the GC M15 suggests the presence of a stellar cusp in the inner part, at least down to distances of a few 10^{-2} pc (Dull et al. 1997). M15 may thus harbor an IMBH (Gerssen et al. 2002; Kiselev et al. 2008) in its center. However, the study on millisecond pulsars in M15 sets an upper limit of $10^3 M_\odot$ on the mass of a hypothetical central BH (De Paolis et al. 1996). In what follows, no central BH is assumed for the modeling of M15.

The observations of M15 by H.E.S.S. were carried out in 2006 and 2007 with an offset angle of 0.7 and zenith angles from 34° to 44° resulting in 15.2 hr of high-quality data at a mean zenith angle of 37.0° . The right-hand side of Figure 1 shows the θ^2 radial distribution of the ON and OFF events for M15. The data analysis reveals no significant gamma-ray signal at the nominal position. With $N_{\text{ON}} = 28$, $N_{\text{OFF}} = 719$, and $\alpha = 26.6$,

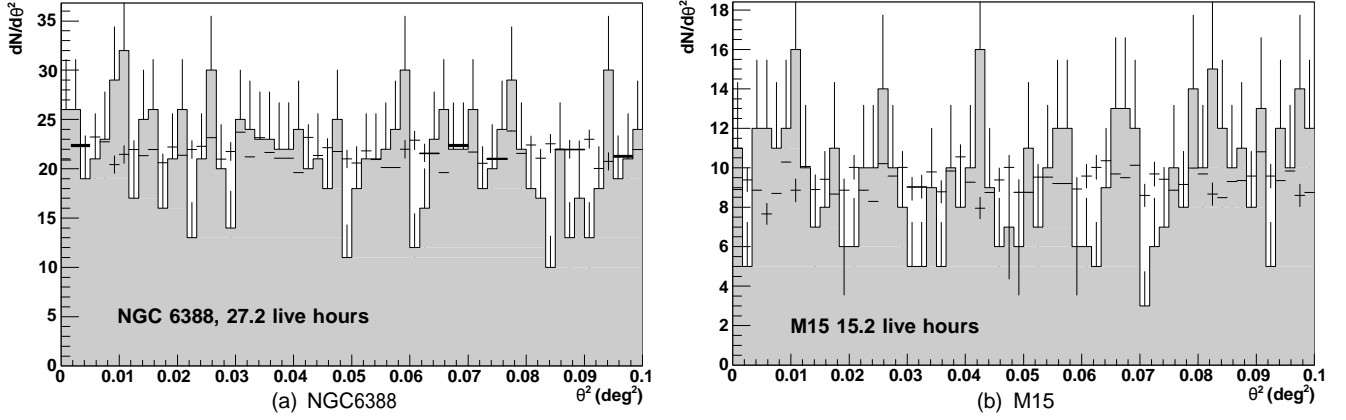


Figure 1. θ^2 radial distribution of the ON (gray histogram) and normalized OFF (black crosses) events for gamma-ray-like events from a 0.07 radius region around the target position for (a) NGC 6388 (R.A. = $17^{\text{h}}36^{\text{m}}17^{\text{s}}.05$ and decl. = $-44^{\circ}44'05''.8$, J2000) and (b) M15 (R.A. = $21^{\text{h}}28^{\text{m}}58^{\text{s}}.3$ and decl. = $12^{\circ}10'00''.6$, J2000). The ON regions correspond to a maximum θ^2 of 0.005 deg^2 . No significant excess is found in the ON region for NGC 6388 or M15.

Table 2
Properties of the NGC 6388 and M15 Globular Clusters Used in This Study

Globular Cluster Name	NGC 6388	M15
Other name	/	NGC 7078
R.A., decl. coordinates (J2000)	$17^{\text{h}}36^{\text{m}}17^{\text{s}}.05, -44^{\circ}44'05''.8$	$21^{\text{h}}28^{\text{m}}58^{\text{s}}.3, 12^{\circ}10'00''.6$
Galactic coordinates (l, b)	$345^{\circ}.55, -6^{\circ}.73$	$64^{\circ}.8, -27^{\circ}.1$
Distance (kpc)	11.5^{a}	10.0^{b}
Core radius r_c (pc)	0.4^{a}	0.04^{c}
Tidal radius r_t (pc)	25^{a}	30^{b}
Estimated mass (M_{\odot})	10^6	5×10^5
Core stellar density ($M_{\odot} \text{ pc}^{-3}$)	5×10^5	10^7
Central velocity dispersion v_{rms} (km s^{-1})	$18.9 \pm 0.8^{\text{d}}$	$10.2 \pm 1.4^{\text{c}}$

Notes.

- ^a Lanzoni et al. (2007).
- ^b Wood et al. (2008).
- ^c Dull et al. (1997).
- ^d Pryor & Meylan (1993).

Table 3

Exposure Time, Mean Zenith Observation Angle, Number of ON Events, Number of OFF Events, α Ratio, and 95% C.L. Upper Limits on the Number of Gamma-rays from the H.E.S.S. Observations for NGC 6388 and M15, Respectively

Globular Cluster Name	NGC 6388	M15
Exposure time ^a (hr)	27.2	15.2
Mean zenith observation angle	$22^{\circ}.9$	$37^{\circ}.0$
N_{ON}	75	28
N_{OFF}	1754	719
α	26.5	26.6
$N_{\gamma}^{95\% \text{ C.L.}}$	21.6	11.5

Notes. See the text for more details.

^a After quality selection.

the expected number of background events in the ON region is 27.0. The 95% C.L. upper limit on the number of gamma-rays is $N_{\gamma}^{95\% \text{ C.L.}} = 11.5$. Table 3 summarizes observations and upper limits on count numbers for NGC 6388 and M15.

3. DARK MATTER CONSTRAINTS

3.1. Dark Matter Halo Modeling

The relaxation time, defined in Equation (A1) of the Appendix, has a much smaller value, $T_r \sim 10^7 \text{ yr}$, in GCs than in

galaxies, where it is typically of the order of 10^{13} yr (Binney & Tremaine 1987). Since GCs are among the oldest objects known, their present DM density depends on their history and evolution. During infall events such as core collapses (Spitzer 1987), the DM is compressed toward the center following the AC scenario (Zel'dovich et al. 1980; Blumenthal et al. 1986). This profile is referred to hereafter as the AC Navarro–Frenk–White (NFW) profile. But the kinetic heating of DM particles by stars (Merritt 2004) tends to wash out the AC effect over a timescale of the order of T_r . Both effects were taken into account in the modeling of M15 and NGC 6388, following the approach of Merritt et al. (2007) and Bertone & Fairbairn (2008).

As mentioned in the introduction, the primordial formation scenario of GCs (Peebles 1984) assumed here requires that GCs were formed in extended DM halos. The DM halo profile of a GC is thus modeled assuming an initial NFW profile (Navarro et al. 1997) described by

$$\rho(r) = \rho_0 \frac{r}{r_s}^{-1} \left(1 + \frac{r}{r_s} \right)^{-2}. \quad (1)$$

This DM halo is parameterized by a virial mass³⁹ M_{vir} and a concentration parameter c_{vir} . The normalization parameter ρ_0

³⁹ M_{vir} is defined as the mass inside the radius R_{vir} assuming a mean density equal to 200 times the critical density of the universe (Amsler et al. 2008).

Table 4

Values of the LOS-integrated Squared Density Averaged Over the Solid Angle (\bar{J}) Expressed in Units of 10^{24} GeV 2 cm $^{-5}$, for the Different DM Halo Profiles

DM Halo Profile Name	NGC 6388	M15
Initial NFW ($M_{\text{vir}}, c_{\text{vir}}$)	2.1 ($10^7 M_{\odot}, 60$)	1.5 ($10^7 M_{\odot}, 50$)
AC NFW	1.3×10^4	4.3×10^3
IMBH NFW	2.2×10^4	/
Final	68	14

Notes. The integration solid angle is $\Delta\Omega = 5 \times 10^{-6}$ sr. The virial mass and concentration for the initial NFW profiles are given in parentheses.

and the scale radius r_s can be related to the virial mass and the concentration parameter using the following relations (Navarro et al. 1997):

$$\rho_0 = \frac{M_{\text{vir}}}{4\pi r_s^3 f(c_{\text{vir}})}, \quad r_s = \frac{R_{\text{vir}}}{c_{\text{vir}}}, \quad (2)$$

where the function $f(x)$ is, neglecting constants, the volume integral of the NFW profile given by $f(x) \equiv \ln(1+x) - x/(1+x)$. The present baryonic mass of the GC provides a lower bound on its virial mass. Besides, for M_{vir} larger than $10^8 M_{\odot}$ the GC would be expected to spiral toward the center of the Milky Way in less than the age of the universe. Conservative values for M_{vir} lie therefore in the range $[5 \times 10^6 - 5 \times 10^7] M_{\odot}$ (Wood et al. 2008), corresponding⁴⁰ to c_{vir} between ~ 48 and 65. In this paper, initial DM halos of GCs are modeled with $M_{\text{vir}} = 10^7 M_{\odot}$. The value of c_{vir} used in the model of NGC 6388 is calculated from the formula of Bullock et al. (2001). For M15, the value of c_{vir} is taken from Wood et al. (2008). Both values are listed in Table 4.

The presence of a central BH changes the DM and stellar densities in regions where the BH dominates the gravitational potential, i.e., for distances to the BH lower than the radius of gravitational influence r_h .⁴¹ The adiabatic growth of the BH leads to a spiked DM distribution with an index of 9/4 for an initial DM distribution with an index of 1, as for the NFW profile. This profile is referred to as the IMBH NFW profile. The spike is smoothed by the kinetic heating of DM by stars over the timescale T_r , forming a density profile proportional to $r^{-3/2}$ called DM crest (Merritt et al. 2007), which corresponds to the final profile.

The dark halo models of M15 and NGC 6388 are described in detail in the Appendix. The DM halo of M15 differs from the model published in Wood et al. (2008), since the effect of DM heating by stars is considered in addition to the effect of AC. The inferred DM mass densities of NGC 6388 and M15 are shown in Figures 2 and 3, respectively.

3.2. Dark Matter Annihilation Signal

The gamma-ray flux expected from DM annihilations can be decomposed into an astrophysical term and a particle physics term as (Bertone et al. 2005)

$$\frac{d\Phi(\Delta\Omega, E_{\gamma})}{dE_{\gamma}} = \frac{1}{8\pi} \frac{(\sigma v)}{m_{\text{DM}}^2} \frac{dN_{\gamma}}{dE_{\gamma}} \times \underbrace{\bar{J}(\Delta\Omega)\Delta\Omega}_{\text{Astrophysics}}. \quad (3)$$

Particle Physics

⁴⁰ M_{vir} and c_{vir} are strongly correlated (Navarro et al. 1997; Bullock et al. 2001). In Bullock et al. (2001), $c_{\text{vir}} = 9 \times (M_{\text{vir}} / 1.5 \times 10^{13} h^{-1} M_{\odot})^{-0.13}$, where h is the present-day normalized Hubble constant (Amsler et al. 2008).

⁴¹ The radius of gravitational influence of a BH is defined by the equation $M(< r_h) \equiv \int_0^{r_h} \rho(r) 4\pi r^2 dr = 2M_{\text{BH}}$.

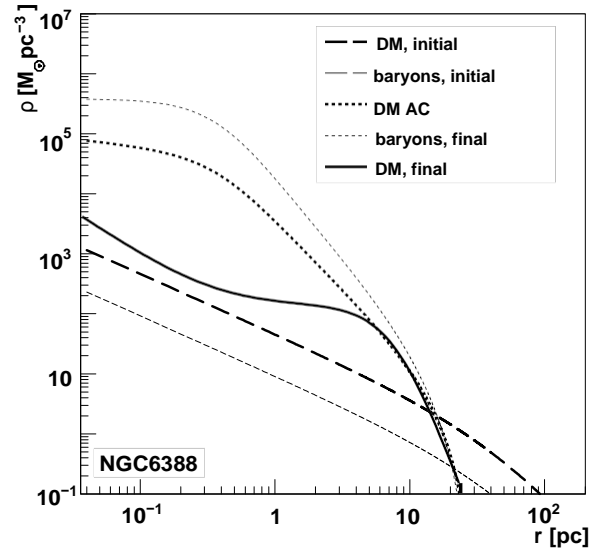


Figure 2. DM and baryonic mass density distributions in NGC 6388. The DM density before (thick dashed line) and after (thick dotted line) the AC by baryons is shown. The initial DM distribution follows an NFW profile with $M_{\text{vir}} = 10^7 M_{\odot}$. The initial (thin dashed line) and final (thin dotted line) baryonic densities are displayed. The final DM density distribution after the effects of the adiabatic growth of the IMBH at the center of NGC 6388 and the kinetic heating by stars is presented (thick solid line). See the text for more details.

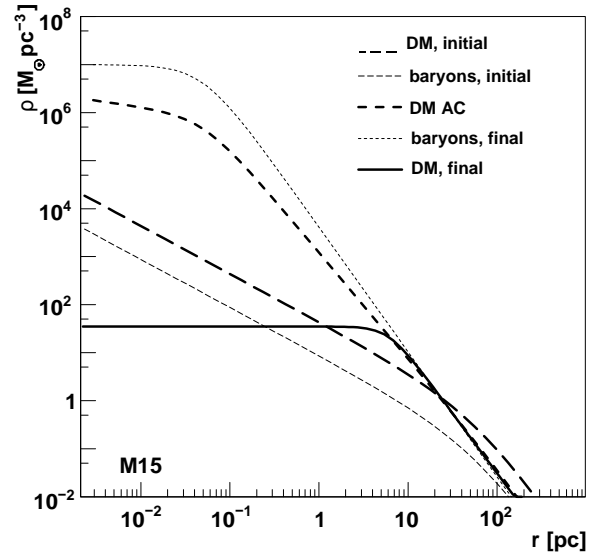


Figure 3. DM and baryonic mass density distributions in M15. The DM density before (thick dashed line) and after (thick dotted line) the AC by baryons is shown. The initial DM distribution follows an NFW profile with $M_{\text{vir}} = 10^7 M_{\odot}$. The initial (thin dashed line) and final (thin dotted line) baryonic densities are displayed. The final DM density distribution after the effect of the kinetic heating by stars is presented (thick solid line). See the text for more details.

The astrophysical factor (\bar{J}) is generally expressed as the integral over the line of sight (LOS) of the squared density averaged over the solid angle $\Delta\Omega$:

$$\bar{J} = \frac{1}{\Delta\Omega} \int_{\Delta\Omega} d\Omega \int_{\text{LOS}} ds \rho^2(r(s)), \quad (4)$$

with $r(s) = \sqrt{\frac{s^2}{s^2 + s_0^2}}$, where $s_0 = 2s_s \cos \theta$, s the distance of the source from the Sun and θ the opening angle of the integration cone centered on the target position. To match the analysis cuts used in

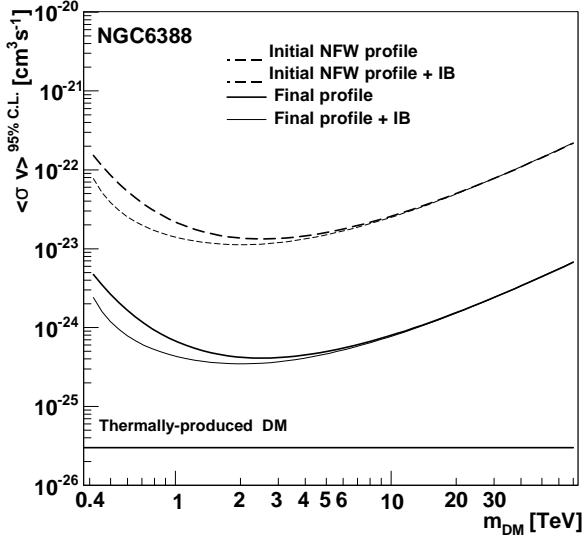


Figure 4. H.E.S.S. upper limits at 95% C.L. on the velocity-weighted annihilation cross section (σv) vs. the DM mass m_{DM} for the Galactic GC NGC 6388. DM halo profiles shown here correspond to the initial NFW profile (dashed thick line) and the realistic profile taking into account plausible astrophysical effects (solid thick line). The contribution from internal bremsstrahlung and final state radiation to the annihilation spectrum is also shown (dashed/solid thin lines) for both profiles. The natural value of (σv) for thermally produced DM is also displayed (long-dashed line).

this work (see Section 2), $\Delta\Omega$ is set to 5×10^{-6} sr. Table 4 shows the values of the astrophysical factor for the DM halo profiles presented in Section 3.1. In the case of the IMBH NFW and final DM profiles for NGC 6388, the calculation of the astrophysical factor requires a minimum cutoff for the integration radius. For the IMBH NFW and final profiles, the integral diverges as $r_{\text{min}}^{-3/2}$ and $\log(r_{\text{min}}^{-1})$, respectively, where r_{min} is the inner radius. r_{min} is usually taken as $\text{Max}[r_S, r_A]$, where $r_S \equiv 2GM_{\text{BH}}/c^2$ is the Schwarzschild radius of the BH and r_A is the self-annihilation radius calculated for an annihilation time of 10 Gyr. Typical values of m_{DM} and (σv) give $r_A \sim 10^{-5}$ pc so that $r_{\text{min}} = r_A$. The value of the astrophysical factor for the final profile is insensitive to the assumed value of r_{min} . The values for M15 are calculated using the DM modeling described in Section 3.1. The evolution of M15 leads to a depletion of DM, implying a decrease of \bar{J} . In the case of NGC 6388, the effect of the BH in the stellar environment boosts \bar{J} to a value higher than that obtained for the initial NFW profile.

3.3. Exclusion Limits

The exclusion limits on the particle physics parameters, i.e., the DM particle mass m_{DM} and the velocity-weighted annihilation cross section (σv), are calculated using the astrophysical factor calculated for each DM halo model by

$$(\sigma v)_{\text{min}}^{95\% \text{ C.L.}} = \frac{8\pi}{T_{\text{obs}} \bar{J}(\Delta\Omega)\Delta\Omega} \frac{m_{\text{DM}}^2}{0} \frac{N_{\gamma}^{95\% \text{ C.L.}}}{A_{\text{eff}}(E_{\gamma}) \frac{dN_{\gamma}}{dE_{\gamma}} dE_{\gamma}}, \quad (5)$$

where dN_{γ}/dE_{γ} is the DM-produced differential continuum gamma-ray spectrum and A_{eff} is the effective area of the instrument during the observations (Aharonian et al. 2008). Figure 4 shows the 95% C.L. exclusion limits for NGC 6388 on (σv) for the initial NFW (dashed line) and the final profile (solid line) derived from the 95% C.L. upper limit on the number of gamma-rays. The generic parameterization from Bergström

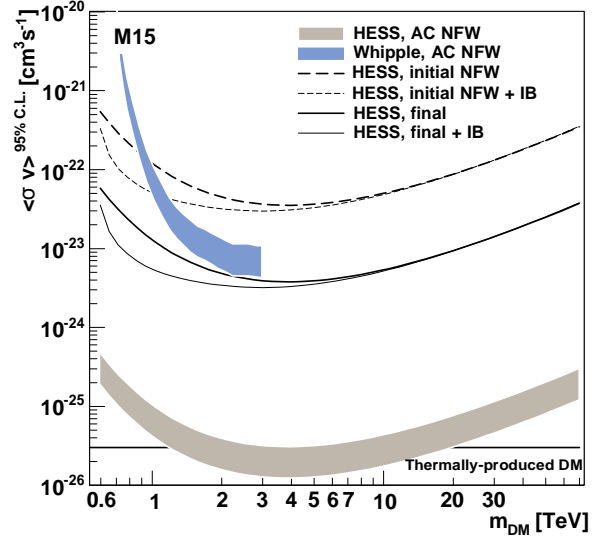


Figure 5. H.E.S.S. upper limits at 95% C.L. on the velocity-weighted annihilation cross section (σv) vs. the DM mass m_{DM} for the Galactic GC M15. Three DM halos are shown: the initial NFW profile (dashed thick/thin line), the NFW profile after DM AC by baryons (AC NFW) used in Wood et al. (2008, gray area), and the final DM profile (solid thick/thin line). The effect of internal bremsstrahlung is also presented (thin dashed/solid lines). The Whipple exclusion limits extracted from Wood et al. (2008) are also plotted (blue area). The natural value of (σv) for thermally produced DM is shown (long-dashed line). (A color version of this figure is available in the online journal.)

et al. (1998) as well as a parameterization including contributions from virtual internal bremsstrahlung and final state radiation (Bringmann et al. 2008) are used for the differential gamma-ray spectra. The Bergström et al. (1998) parameterization is derived from a fit to the gamma-ray spectrum from neutralino annihilations into W and Z pairs. The latter includes both gamma-rays from virtual particles and from charged particle final states of the pair annihilation of winos (Bertone et al. 2005). The limits are one to three orders of magnitude above the natural value of the velocity-weighted annihilation cross section for thermally produced DM (Bertone et al. 2005). Figure 5 shows the H.E.S.S. 95% C.L. exclusion limits for M15 for the initial and final DM profiles, as well as those obtained with the Whipple Cerenkov telescope (blue area) in Wood et al. (2008). The thickness of the drawn lines represents the astrophysical uncertainty induced by the plausible mass range for the initial virial mass. The H.E.S.S. limit reaches $(\sigma v) \sim 5 \times 10^{-23}$ cm 3 s $^{-1}$ and $(\sigma v) \sim 5 \times 10^{-24}$ cm 3 s $^{-1}$ around $m_{\text{DM}} = 2$ TeV for the initial NFW profile and the final profile, respectively. For comparison, the exclusion limit obtained for H.E.S.S. using the DM halo modeling of Wood et al. (2008) is also shown (gray area). Stronger constraints are obtained with H.E.S.S. due to the combination of larger effective area, 3×10^5 m 2 versus 5×10^4 m 2 , better angular resolution, $0'.06$ versus $0'.25$, better upper limit on the number of gamma-rays (11.5 versus ~ 67.7), and longer observation time (15.2 hr versus 1.2 hr).

4. SUMMARY

The present paper gives for the first time exclusion limits on DM toward several GCs taking into account all relevant astrophysical effects affecting the hypothetical DM halo. The H.E.S.S. observations reveal no significant gamma-ray excess from point-like sources located at the nominal position of the Galactic GCs NGC 6388 and M15. The hypothetical DM halo

has been modeled taking into account possible astrophysical processes leading to substantial changes in the initial DM profile: the AC of DM by baryons and the adiabatic growth of a BH at the center of the DM halo. The scattering of DM by stars in such a dense stellar environment has been taken into account to provide realistic final DM halos. This effect is of crucial importance to model DM halos in these baryon-dominated environments and leads to a depletion of DM during the evolution of the GC. On the other hand, the presence of a central massive BH enhances the DM density in the center. The constraints on the velocity-weighted annihilation cross section of the DM particle are derived using DM halo profiles taking into account the above-mentioned astrophysical effects on the initial DM density. They lie at the level of a few $10^{-25} \text{ cm}^3 \text{ s}^{-1}$ for NGC 6388 in the TeV energy range. Assuming the absence of a massive BH in the center of M15, the constraints are of the order of a few $10^{-24} \text{ cm}^3 \text{ s}^{-1}$.

The support of the Namibian authorities and of the University of Namibia in facilitating the construction and operation of H.E.S.S. is gratefully acknowledged, as is the support by the German Ministry for Education and Research (BMBF), the Max Planck Society, the French Ministry for Research, the CNRS-IN2P3 and the Astroparticle Interdisciplinary Programme of the CNRS, the U.K. Particle Physics and Astronomy Research Council (PPARC), the IPNP of the Charles University, the South African Department of Science and Technology and National Research Foundation, and the University of Namibia. We appreciate the excellent work of the technical support staff in Berlin, Durham, Hamburg, Heidelberg, Palaiseau, Paris, Saclay, and Namibia in the construction and operation of the equipment.

APPENDIX MODELS OF THE M15 AND NGC 6388 DARK MATTER HALOS

A.1. M15 Dark Matter Halo

The modeling of the M15 DM halo proceeds in two steps. In the first step, the dark halo is assumed to be adiabatically compressed during the collapse of the core of M15. The model used for the initial and final baryon and DM densities is described in Wood et al. (2008). The final baryon density is the observed mass density taken from Gebhardt et al. (1997). The DM is compressed during the baryonic collapse. The timescale for the collapse is $\sim 100 T_r$, where the relaxation time T_r is given by Spitzer (1987):

$$T_r = \frac{3.4 \times 10^9}{\ln \Lambda} \left(\frac{v_{\text{rms}}}{\text{km s}^{-1}} \right)^3 \frac{m}{M_\odot}^{-2} \frac{n}{\text{pc}^{-3}}^{-1} \text{ yr.} \quad (\text{A1})$$

In Equation (A1), v_{rms} is the velocity dispersion, n is the stellar density, and $\ln \Lambda$ is the usual Coulomb logarithm. In the case of the center of M15, taking $v_{\text{rms}} = 10.2 \pm 1.4 \text{ km s}^{-1}$ (Dull et al. 1997), $\ln \Lambda = 13.1$, and adopting a typical stellar mass value of $m = 0.4 M_\odot$ (Dull et al. 1997), one finds $T_r \sim 7 \times 10^4 \text{ yr}$. T_r is an increasing function of the distance r to the center of the M15. For $r \gtrsim r_{\text{heat}} = 5 \text{ pc}$, the relaxation time is larger than the age of the universe. The central value of T_r and the position of r_{heat} have only weak dependences on the actual values of v_{rms} and n when the latter are varied in their uncertainty ranges. Because of AC, the DM evolution takes place in less than a few orbital periods. The orbital period of a star orbiting the core

of M15 is of the order of 1000 yr, which is much less than T_r . The AC method should thus be valid. The value of the DM density after AC is similar to the result of Wood et al. (2008), see Figure 3 and Figure 7 of Wood et al. (2008). At the same time, the DM is heated up by stellar matter. This process is described in Merritt (2004). DM is scattered by stars in a few T_r , leading to a depletion of the core. For $r \gtrsim 5 \text{ pc}$, the DM distribution is not affected by heating. The DM scattering is taken into account with the procedure described in Bertone & Fairbairn (2008) for the GC M4. A DM mass density of $\rho_{\text{M15}} \sim 35 M_\odot \text{ pc}^{-3}$ is obtained at the radius where the heating time is comparable to the age of the universe. For $r \gtrsim 5 \text{ pc}$, the DM halo is swept out by heating and the DM mass density was assumed to take the constant ρ_{M15} value. The DM mass density of M15 called final profile is shown in Figure 3.

A.2. NGC 6388 Dark Matter Halo

The modeling of the NGC 6388 DM halo also proceeds in two steps. The first step is the AC of the DM halo by the IMBH and baryons. An initial baryon fraction of 20% (Spergel et al. 2007) is assumed with the same spatial distribution like the DM. The AC scenario gives the resulting DM distribution knowing the measured baryonic mass profile. This DM halo profile is called AC NFW profile. The surface density profile of NGC 6388 is well fitted by a modified King model including a BH, characterized by a core radius $r_c = 7.2$ and a concentration $c = 1.8$ (Lanzoni et al. 2007). Using these parameters, the numerical integration of the Poisson equation yields the behavior of the gravitational potential from which it is straightforward to compute the baryonic density profile. The initial NFW profile is characterized by $M_{\text{vir}} = 10^7 M_\odot$. Since the mass of the IMBH is just a small fraction of the total mass in the core of NGC 6388, the dynamics of DM is influenced mainly by baryonic matter, except in the immediate vicinity of the BH. Using a central velocity dispersion of $v_{\text{rms}} = 18.9 \pm 0.8 \text{ km s}^{-1}$ (Pryor & Meylan 1993) and $\ln \Lambda = 14.7$, the central relaxation time is found to be $T_r \sim 8 \times 10^6 \text{ yr}$. The orbital period of a star orbiting the core of NGC 6388 is 5000 yr, so that the AC method is again valid. The relaxation time is larger than the age of the universe for $r > r_{\text{heat}}$. The distribution of the DM density around the BH (for $r \gtrsim r_h$) is changing with time, but tends to a power law with index $3/2$ after a few T_r . The final DM distribution is thus obtained by extending the prescription of Bertone & Fairbairn (2008). Far from the center of the cluster, the stellar density is low and thus the heating time becomes large so that the DM distribution is unaffected. A mass density of $\sim 140 M_\odot \text{ pc}^{-3}$ is obtained at the radius $r_{\text{heat}} \sim 4 \text{ pc}$ where the heating time is comparable to the age of the universe. In the region $r_h < r < r_{\text{heat}}$, the DM density is expected to be described by a smooth curve similar to Figure 1 of Merritt et al. (2007). In the modeling for NGC 6388, the DM density was conservatively assumed to take a constant value of $140 M_\odot \text{ pc}^{-3}$ in the region $r_h < r < r_{\text{heat}}$. For $r < r_h$, the DM density is given by $\rho(r) = 140 M_\odot \text{ pc}^{-3} (r/r_h)^{-3/2}$. The final profile for the DM distribution of NGC 6388 is shown in Figure 2. At the position of NGC 6388, the DM density from the smooth Galactic halo assuming an NFW profile is $\sim 0.03 M_\odot \text{ pc}^{-3}$.

REFERENCES

- Aharonian, F., et al. (HESS Collaboration). 2005, *A&A*, **430**, 865
 Aharonian, F., et al. (HESS Collaboration). 2006a, *Phys. Rev. Lett.*, **97**, 221102 (erratum 97, 249901)
 Aharonian, F., et al. (HESS Collaboration). 2006b, *A&A*, **457**, 899

- Aharonian, F., et al. (HESS Collaboration). 2008, *Astropart. Phys.*, **29**, 55 (erratum 33, 174 [2010])
- Aharonian, F., et al. (HESS Collaboration). 2009a, *A&A*, **503**, 817
- Aharonian, F., et al. (HESS Collaboration). 2009b, *ApJ*, **691**, 175
- Aharonian, F., et al. (HESS Collaboration). 2009c, *A&A*, **499**, 273
- Aharonian, F., et al. (HESS Collaboration). 2011, *Astropart. Phys.*, **34**, 608
- Amsler, C., et al. (Particle Data Group). 2008, *Phys. Lett. B*, **667**, 1
- Anderhub, H., et al. (MAGIC Collaboration). 2009, *ApJ*, **702**, 266
- Baumgardt, H., Makino, J., & Hut, P. 2005, *ApJ*, **620**, 238
- Baumgardt, H., et al. 2009, *MNRAS*, **396**, 2051
- Berge, D., Funk, S., & Hinton, J. 2007, *A&A*, **466**, 1219
- Bergström, L., Ullio, P., & Buckley, J. 1998, *Astropart. Phys.*, **9**, 137
- Bertone, G., & Fairbairn, M. 2008, *Phys. Rev. D*, **77**, 043515
- Bertone, G., Hooper, D., & Silk, J. 2005, *Phys. Rep.*, **405**, 279
- Binney, J., & Tremaine, S. 1987, *Galactic Dynamics* (Princeton, NJ: Princeton Univ. Press), 747
- Blumenthal, G. R., Faber, S. M., Flores, R., & Primack, J. R. 1986, *ApJ*, **301**, 27
- Bringmann, T., Bergstrom, L., & Edsjo, J. 2008, *J. High Energy Phys.*, **JHEP01(2008)049**
- Brodie, J. P., & Strader, J. 2006, *ARA&A*, **44**, 193
- Bullock, J. S., Kolatt, T. S., Sigad, Y., Somerville, R. S., Kravtsov, A. V., Klypin, A. A., Primack, J. R., & Dekel, A. 2001, *MNRAS*, **321**, 559
- Cohen, J. G., Kirby, E. N., Simon, J. D., & Geha, M. 2010, *ApJ*, **725**, 288
- Colbert, E., & Ptak, A. 2002, *ApJS*, **143**, 25
- Conroy, C., Loeb, A., & Spergel, D. 2010, arXiv:1010.5783
- de Naurois, M., & Rolland, L. 2009, *Astropart. Phys.*, **32**, 231
- De Paolis, F., Gurzadian, V. G., & Ingrassio, G. 1996, *A&A*, **315**, 396
- Dewangan, G. C., Griffiths, R. E., Choudhury, M., Miyaji, T., & Schurch, N. J. 2005, *ApJ*, **635**, 198
- Dull, J. D., Cohn, H. N., Lugger, P. M., Murphy, B. W., Seitzer, P. O., Callanan, P. J., Rutten, R. G. M., & Charles, P. A. 1997, *ApJ*, **481**, 267
- Englmaier, P., & Gerhard, O. 2005, *BAAS*, **37**, 513
- Gebhardt, K., Pryor, C., Williams, T. B., Hesser, J. E., & Stetson, P. B. 1997, *AJ*, **113**, 1026
- Gerssen, J., van der Marel, R. P., Gebhardt, K., Guhathakurta, P., Peterson, R. C., & Pryor, C. 2002, *AJ*, **124**, 3270
- Gnedin, O. Y., Kravtsov, A. V., Klypin, A. A., & Nagai, D. 2004, *ApJ*, **616**, 16
- Gnedin, O. Y., & Primack, J. R. 2004, *Phys. Rev. Lett.*, **93**, 061302
- Gondolo, P., & Silk, J. 1999, *Phys. Rev. Lett.*, **83**, 1719
- Harris, W. E. 1996, *AJ*, **112**, 1487 (2010 December update)
- Islam, R., Taylor, J., & Silk, J. 2004, *MNRAS*, **354**, 443
- Jesseit, R., Naab, T., & Burkert, A. 2002, *ApJ*, **571**, L89
- Kabuki, S., et al. (CANGAROO Collaboration). 2007, *ApJ*, **668**, 968
- Kiselev, A. A., et al. 2008, *Astron. Lett.*, **34**, 529
- Komatsu, E., et al. (WMAP Collaboration). 2009, *ApJS*, **180**, 330
- Kong, A. K. H. 2007, *ApJ*, **668**, L139
- Koushiappas, S. M., Bullock, J. S., & Dekel, A. 2004, *MNRAS*, **354**, 292
- Lanzoni, B., et al. 2007, *ApJ*, **668**, L139
- Magorrian, J., et al. 1998, *AJ*, **115**, 2285
- Mateo, M. 1998, *ARA&A*, **36**, 435
- McCutcheon, M. (VERITAS Collaboration) 2009, Proc. 31st Int. Cosmic Ray Conf. (ICRC), Lodz, Poland, 2009 July (arXiv:0907.4974)
- Merritt, D. 2004, *Phys. Rev. Lett.*, **92**, 201304
- Merritt, D., Harfst, S., & Bertone, G. 2007, *Phys. Rev. D*, **75**, 043517
- Navarro, J. F., Frenk, C. S., & White, S. D. M. 1997, *ApJ*, **490**, 493
- Noyola, E., & Gebhardt, K. 2006, *AJ*, **132**, 447
- Noyola, E., Gebhardt, K., & Bergmann, M. 2008, *ApJ*, **676**, 1008
- Nucita, A. A., De Paolis, F., Ingrassio, G., Carpano, S., & Guainazzi, M. 2008, *A&A*, **478**, 763
- Peebles, P. J. E. 1984, *ApJ*, **277**, 470
- Prada, F., Klypin, A., Flix, J., Martinez, M., & Simonneau, E. 2004, *Phys. Rev. Lett.*, **93**, 241301
- Pryor, C., & Meylan, G. 1993, in ASP Conf. Ser. 50, Structure and Dynamics of Globular Clusters, ed. S. G. Djorgovski & G. Meylan (San Francisco, CA: ASP), 357
- Pühlhofer, G., et al. (HEGRA Collaboration). 2003, *Astropart. Phys.*, **20**, 267
- Rolke, W. A., Lopez, A. M., & Conrad, J. 2005, *Nucl. Instrum. Methods Phys. Res. A*, **551**, 493
- Spergel, D. N., et al. (WMAP Collaboration). 2007, *ApJS*, **170**, 377
- Spitzer, L. 1987, *Dynamical Evolution of Globular Clusters* (Princeton, NJ: Princeton Univ. Press), 191
- Swartz, D. A., Ghosh, K. K., Tennant, A. F., & Wu, K. W. 2004, *ApJS*, **154**, 519
- Ulvestad, J. S., Greene, J. E., & Ho, L. C. 2007, *ApJ*, **661**, L151
- Umbreit, S., Fregeau, J. M., & Rasio, F. A. 2008, *Proc. IAU Symp.*, **246**, 351
- Volonteri, M., Haardt, F., & Madau, P. 2003, *ApJ*, **582**, 559
- Wood, M., et al. 2008, *ApJ*, **678**, 594
- Yungelson, L. R., van den Heuvel, E. P. J., Vink, J. S., Portegies Zwart, S. F., & de Koter, A. 2008, *A&A*, **477**, 223
- Zel'dovich, Y. B., Klypin, A. A., Khlopov, M. Y., & Chechetkin, V. M. 1980, *Sov. J. Nucl. Phys.*, **31**, 664 (*Yad. Fiz.*, **31**, 1286)